A laser pump-re-pump atomic magnetometer*

Yang Ai-Lin(杨爱林), Yang Guo-Qing(杨国卿), Cai Xun-Ming(蔡勋明),
Xu Yun-Fei(徐云飞), and Lin Qiang(林 强)†

Institute of Optics, Department of Physics, Zhejiang University, Hangzhou 310027, *China*

(Received 27 November 2012; revised manuscript received 9 May 2013)

We demonstrate experimentally an atomic magnetometer based on optical pumping theory, a magnetic resonance that is induced by a radio frequency field and dependent on the magnetic field strength. Compared with the conventional method using one radiation field, which is used not only as the probe beam but also as a pump beam, the additional re-pump beam can increase remarkably the amplitude of the signal. It is shown that the amplitude of the magnetic field resonance signal can increase more than 55% by using an additional re-pump beam, which makes the sensitivity of the magnetometer higher. Finally, we investigate the relation between amplitude of the signal and re-pump laser power, and calculate the atomic population in the trapping states with rate equations.

Keywords: atomic magnetometer, optical pumping, sensitivity

PACS: 07.55.Ge, 76.70.Hb, 33.80.Be, 42.62.Eh **DOI:** 10.1088/1674-1056/22/12/120702

1. Introduction

High-density hot alkali-metal vapors are used in vital metrology applications in geophysical surveying, space science, nuclear magnetic resonance, non-destructive testing, medical diagnoses, gravitational wave detection, etc.[1–15] In these applications the resolution of frequency measurement of the hyperfine or Zeeman resonance can be improved by increasing the number of alkali-metal atoms. The present work presents a highly sensitive rubidium atomic magnetometer based on laser optical pumping. The technique of optical pumping, developed more than half a century ago, is a powerful means for the generation of a high degree of spin polarization in dilute atomic vapors,[16] and can be used to measure magnetic field.[17] It is known that a sample of alkali-metal atoms can be polarized along a given axis by optically pumping it along that axis with circularly polarized light. When special precautions are taken to preserve a long lifetime of the sample's spin polarization, any perturbations of this polarization, for example, those induced by external magnetic fields, can be detected with extreme sensitivity. Compared with the conventional amalgam vapor lamp magnetometer, the diode laser pumped alkali magnetometer has significant advantages.[18] As is well known, the fiber optics are non-magnetic, and an optic fiber coupled device allows flexible location of the instrument without magnetic interference. Diode laser is an easier and more efficient couple to optical fiber due to smaller optical divergence. Also, diode laser has the potential to be battery operated at room temperature, miniaturized, and ruggedized for the development of a compact magnetometer.

The primary goal of this experiment is to study the influence of an additional re-pump laser on the amplitude of the signal. We study the magnetometer based on optical pumping using two circular lights, and we call it a pump-re-pump magnetometer. It is shown that an additional re-pump light can improve the amplitude of the signal efficiently due to a higher atom utilization ratio, and can be a promising method to improve the sensitivity of the magnetometer.

2. Experimental procedure and results

Optically detected magnetic resonance can be understood as a three-step process: optical pumping process, interaction with external fields, and probing process. Firstly, a resonant circularly polarized laser beam creates a spin polarization in the atomic vapor via optical pumping. Next, the atomic magnetic moment experiences a torque due to a magnetic field. Finally, this magnetic field is detected by monitoring the power transmitted through the sample with a photodiode and a lock-in amplifier. The actual magnetometer will be realized in the following way.

Optical pumping is achieved by light from an extended cavity semiconductor laser whose frequency is tuned to ^{87}Rb D1 transition ($\lambda = 795$ nm) with polarization spectroscopy by a vapor cell.[19] Figure 1(a) shows the traditional optical pumping method. A circular beam produces a coherent atomic population in $5S_{1/2}$, $F = 2$ Zeeman magnetic sub-states, but there are still a portion of atoms in the state of $5S_{1/2}$, $F = 1$.

*Project supported by the National Natural Science Foundation of China (Grant Nos. 60925022 and 11104243), the Fundamental Research Funds for the Central Universities, China (Grant No. 2012FZA3001), and the National Key Basic Research and Development Program of China (Grant No. 2013CB329501).

†Corresponding author. E-mail: qlin@zju.edu.cn

© 2013 Chinese Physical Society and IOP Publishing Ltd

A radio frequency field is turned to the splitting of $\Delta m_F = 1$ Zeeman sublevels and then the magnetic resonant signal is detected. Figure 1(a) shows that almost all atoms are trapped in the states $5S_{1/2}$, $F = 2$, $m_F = 1$ and $m_F = 2$ via an additional laser as shown in Fig. 1(b). We prepare the atoms using two optical pumping processes. In the first optical pumping process a circular laser field drives the $5S_{1/2}$, $F = 2 \rightarrow 5P_{1/2}$, $F = 1$ transition and creates spin polarization. In the second optical pumping process a separate laser field drives $5S_{1/2}$, $F = 1 \rightarrow 5P_{1/2}$, $F = 2$ transition, ensuring that all magnetic sub-states in the $5S_{1/2}$, $F = 1$ manifold are emptied because of angular momentum selection rule.

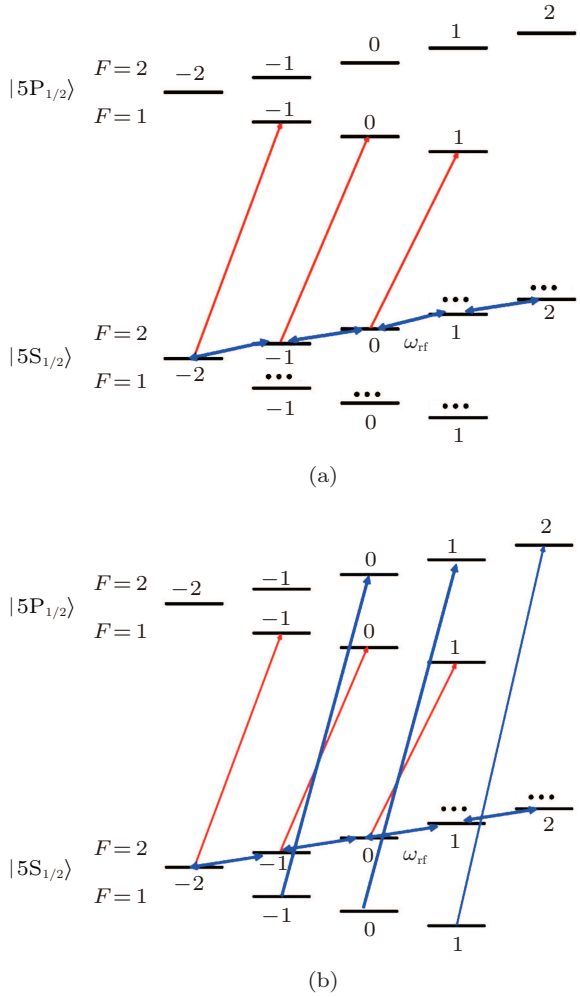


Fig. 1. (color online) Energy level diagrams of ^{87}Rb showing atom transition using (a) a traditional method and (b) the additional re-pump beam scheme.

A diagram of the magnetometer is shown in Fig. 2. In this experiment, the cylinder cell (diameter and length are 2.5 cm and 5 cm respectively), is mounted inside four layers of magnetic shields with a shielding factor of 10^6, filled with natural Rb and a buffer gas containing a mixture of neon at 1333 Pa and argon at 1333 Pa to hinder vapor diffusion to the interaction region. In order to create sufficient atomic density in the small cell, we heat it to 56 °C. A long solenoid is used to create a standard static magnetic field and a shorter one is for modulating the magnetic field. The magnetic fields are parallel to the light and normal to the flat cell. The radio frequency field perpendicular to the light propagation is produced by a pair of quadratic coils of 55-cm radius and their mutual distance is also 55 cm. The laser beam is transported by a single-mode polarization-maintaining optical fiber to the cell, and it is circularly polarized before entering the cell. The power transmitted through the Rb cell is detected via a photodiode. The diameter of the beam at the cell is about 7 mm. The photocurrent is analyzed via a lock-in amplifier by magnetic energy level modulation.[20]

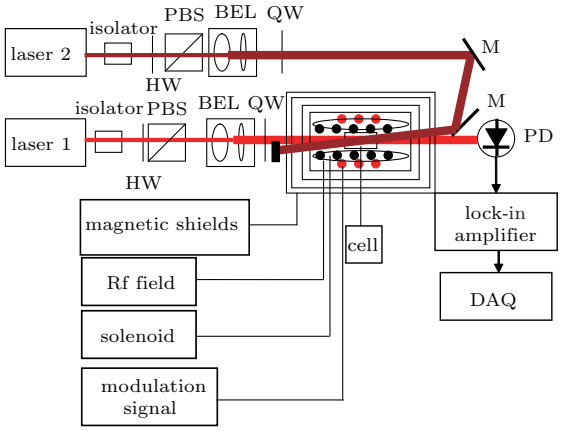


Fig. 2. (color online) Schematic diagram of the experimental setup, where HW denotes the half wave plate, PD the photodiode, QW the quarter wave plate, M the mirror, BS the beam splitter, PBS the polarization beam splitter, BEL the beam expansion lenses, and DAQ the data acquisition.

Figure 3(a) shows a typical absorption spectrum with a full width at half maximum (FWHM) of 1.2 kHz versus radio frequency. Figure 3(b) displays the spectrum recorded from the lock-in amplifier output through energy level modulation scheme, in which the energy levels are modulated by an alternating current magnetic field generated through a solenoid. The magnetic field used in these experiments is nominally 50 mGs (1 Gs = 10^{-4} T), the probe laser was 0.1 mW. The resulting signal from the lock-in amplifier is shown in Fig. 3(c), where the magnetic field varies in steps of 0.7 nT in the 2-s interval, with a time constant of 30 ms, sensitivity of 2 mV, a low-pass roll off of 24 dB/octave.

In Fig. 4, we show the probe light transmittance as a function of radio frequency. The probe and re-pump laser are both 0.1 mW. It is clearly seen from this figure that the amplitude of resonance in the presence of an additional re-pump beam (dashed line) is much larger than the traditional scheme (solid line), and their amplitude ratio is around 7 to 4. In order to determine the best experimental scheme, we study two re-pump

schemes. In this part, we use $5S_{1/2}$, $F = 2 \rightarrow 5P_{1/2}$, $F = 1$ as the probe beam, and $5S_{1/2}$, $F = 1 \rightarrow 5P_{1/2}$, $F = 1$ and $5S_{1/2}$, $F = 1 \rightarrow 5P_{1/2}$, $F = 2$ as the re-pump beam. In Fig. 4, it is clearly shown that the $5S_{1/2}$, $F = 1 \rightarrow 5P_{1/2}$, $F = 2$ is used as the re-pump beam to obtain a larger magnetic field resonance signal.

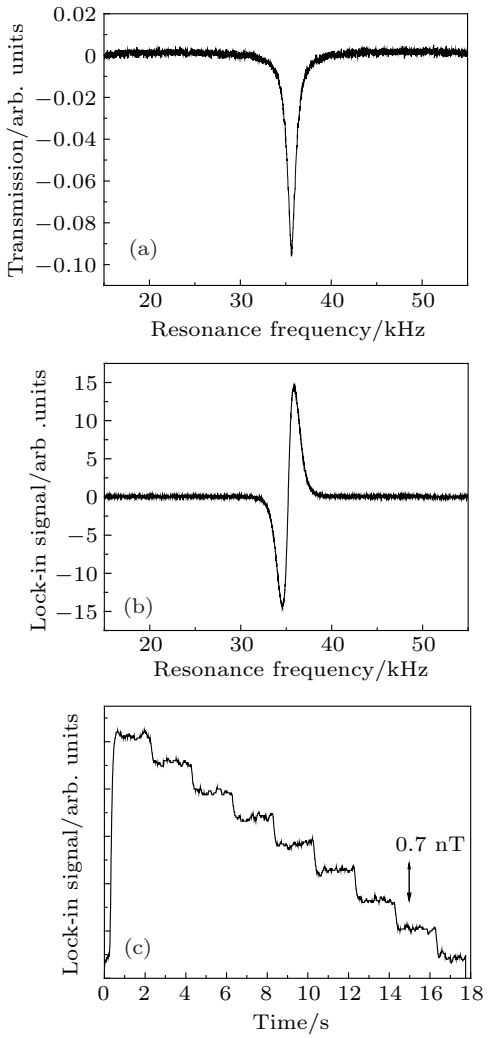


Fig. 3. (a) Absorption spectrum versus radio frequency, (b) lock-in signal versus radio frequency, and (c) lock-in signal versus time as the magnetic field varies in steps of 0.7 nT in each 2-s interval.

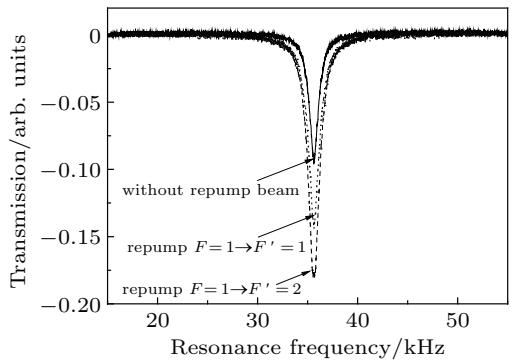


Fig. 4. Comparison among different re-pump schemes.

The results can be explained in physics as follows. Assume the atom number to be a constant. Because we use $5S_{1/2}$, $F = 2$ to $5P_{1/2}$, $F = 1$ as the probe beam, atoms trapping in the state of $5S_{1/2}$, $F = 1$ do not make a contribution to the signal in the absence of the re-pump beam. Furthermore, the re-pump beam using $5S_{1/2}$, $F = 1 \rightarrow 5P_{1/2}$, $F = 2$ is more effective than using $5S_{1/2}$, $F = 1 \rightarrow 5P_{1/2}$, $F = 1$, for which the reason is obvious: $5S_{1/2}$, $F = 1 \rightarrow 5P_{1/2}$, $F = 2$ re-pump beam enables almost all atoms in the states to contribute to the signal, while $5S_{1/2}$, $F = 1 \rightarrow 5P_{1/2}$, $F = 1$ cannot pump atoms in the state $5S_{1/2}$, $F = 1$, $m_F = 1$ for our consideration case.

Figure 5 represents the absorption spectra versus radio frequency for some values of re-pump light power when the probe laser is kept unchanged. In this experiment, we choose $5S_{1/2}$, $F = 2$ to $5P_{1/2}$, $F = 1$ and $5S_{1/2}$, $F = 1 \rightarrow 5P_{1/2}$, $F = 2$ as probe beam and re-pump beam, respectively. The probe beam power is 0.1 mW. It is seen in Fig. 5 that the amplitude of the signal increases with re-pump laser power increasing, e.g. for $I_{\text{repump}} = 0.05$ mW and 0.4 mW, we have $(E_t - E_i)/E_i = 56.3\%$ and 118.8% respectively, where E_t is the amplitude of signal in the presence of a re-pump beam, and E_i is the amplitude of signal in the absence of a re-pump beam.

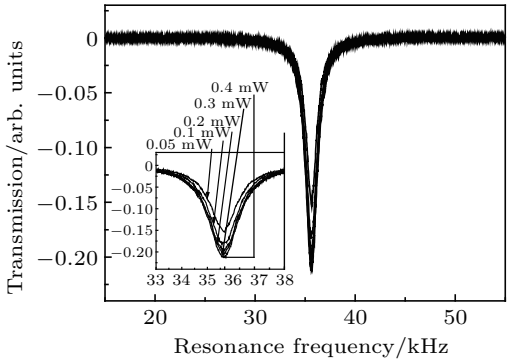


Fig. 5. Absorption spectra versus radio frequency for different values of re-pump light power. The inset shows the magnified transmission dips.

We have discussed that the amplitude of the signal is relevant to the atomic population in the trapping states ($5S_{1/2}$, $F = 2, m_F = 1, 2$). In order to explain our results, we calculate the atomic population in the trapping states with the following simplified model. We use two circular polarization beams corresponding to the transitions from levels $5S_{1/2}$, $F = 2$ to $5P_{1/2}$, $F = 1$ and $5S_{1/2}$, $F = 1$ to $5P_{1/2}$, $F = 2$, respectively. In this consideration case, atoms in $5S_{1/2}$, $F = 1$ ground state may absorb a σ^+ photon because the excited state includes an $m_F = 2$ sublevel; similarly, atoms in $5S_{1/2}$, $F = 2$, $m_F = -2$, –1, 0 may also absorb a σ^+ photon. However, atoms in the $F = 2$, $m_F = 1$, 2 sublevel of the ground state are forbidden from absorbing a photon. The probabilities ρ_1, ρ_2, ρ_3, ρ_4, ρ_5, ρ_6, ρ_7, and ρ_8 describe the number densities in the eight Zeeman sublevels of the ground state as shown in Fig. 6, and their

initial values are all 0.125. The optical pumping rate equations can be written as follows:

$$\begin{aligned}
\dot{\rho}_1 &= -(\gamma_{14}+\gamma_{15}+\gamma_{16}+\gamma_{12})\rho_1+\gamma_{14}\rho_4+\gamma_{15}\rho_5 \\
&\quad +\gamma_{16}\rho_6+\gamma_{12}\rho_2+(\Gamma/8)k-R_{\rm op2}\rho_1, \\
\dot{\rho}_2 &= -(\gamma_{12}+\gamma_{25}+\gamma_{26}+\gamma_{27}+\gamma_{23})\rho_2+\gamma_{12}\rho_1 \\
&\quad +\gamma_{25}\rho_5+\gamma_{26}\rho_6+\gamma_{27}\rho_7+\gamma_{23}\rho_3+(\Gamma/8)k-R_{\rm op2}\rho_2, \\
\dot{\rho}_3 &= -(\gamma_{23}+\gamma_{36}+\gamma_{37}+\gamma_{38})\rho_3+\gamma_{23}\rho_2+\gamma_{36}\rho_6 \\
&\quad +\gamma_{37}\rho_7+\gamma_{38}\rho_8+(\Gamma/8)k-R_{\rm op2}\rho_3, \\
\dot{\rho}_4 &= -(\gamma_{14}+\gamma_{45})\rho_4+\gamma_{14}\rho_1+\gamma_{45}\rho_5+(\Gamma/8)k-R_{\rm op1}\rho_4, \\
\dot{\rho}_5 &= -(\gamma_{45}+\gamma_{56}+\gamma_{15}+\gamma_{25})\rho_5+\gamma_{45}\rho_4+\gamma_{56}\rho_6 \\
&\quad +\gamma_{15}\rho_1+\gamma_{25}\rho_2+(\Gamma/8)k-R_{\rm op1}\rho_5, \\
\dot{\rho}_6 &= -(\gamma_{56}+\gamma_{67}+\gamma_{16}+\gamma_{26}+\gamma_{36})\rho_6+\gamma_{56}\rho_5 \\
&\quad +\gamma_{67}\rho_7+\gamma_{16}\rho_1+\gamma_{26}\rho_2+\gamma_{36}\rho_3+(\Gamma/8)k-R_{\rm op1}\rho_6, \\
\dot{\rho}_7 &= -(\gamma_{67}+\gamma_{78}+\gamma_{27}+\gamma_{37})\rho_7+\gamma_{67}\rho_6+\gamma_{78}\rho_8 \\
&\quad +\gamma_{27}\rho_2+\gamma_{37}\rho_3+(\Gamma/8)k, \\
\dot{\rho}_8 &= -(\gamma_{78}+\gamma_{38})\rho_8+\gamma_{78}\rho_7+\gamma_{38}\rho_3+(\Gamma/8)k, \qquad (1)
\end{aligned}$$

where decay rates γ_{ij} describe the relative population transfer rates between magnetic sublevels of ground states,[16] and Γ denotes the spontaneous rate of decay of atoms from the excited state to the ground state. For simplicity, we assume that the Zeeman sublevels of excited states are degenerate, and the excited atoms have equal probability of decaying to either of the ground-state Zeeman levels. The optical pumping rate $R_{\rm op}$ is defined as the average rate at which an unpolarized atom absorbs a photon from the pump beam, which depends on the intensity of the light.[21,22] In Eq. (1), $k=R_{\rm op1}(\rho_4+\rho_5+\rho_6)$ and $k=R_{\rm op1}(\rho_4+\rho_5+\rho_6)+R_{\rm op2}(\rho_1+\rho_2+\rho_3)$ represent excited state atoms corresponding to one field and two fields, respectively.

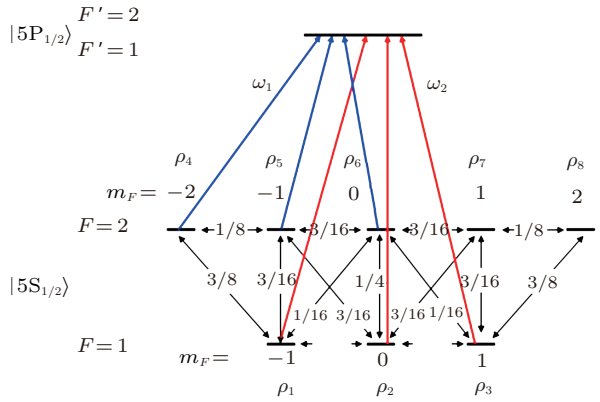


Fig. 6. (color online) Excitation scheme and population-transfer rates between magnetic sublevels of ground states.

We numerically calculate atomic population as a function of the re-pump beam power according to Eq. (1). For simplicity, we let $\Gamma=1$, and all physical quantities are given in the units of Γ. The parameters used here are $\gamma_{12}=\Gamma/160$, $\gamma_{14}=3\Gamma/80$, $\gamma_{15}=3\Gamma/160$, $\gamma_{16}=\Gamma/160$, $\gamma_{23}=\Gamma/160$, $\gamma_{25}=3\Gamma/160$, $\gamma_{26}=\Gamma/40$, $\gamma_{27}=3\Gamma/160$, $\gamma_{36}=\Gamma/160$, $\gamma_{37}=3\Gamma/160$, $\gamma_{38}=3\Gamma/80$, $\gamma_{45}=\Gamma/80$, $\gamma_{56}=3\Gamma/160$, $\gamma_{67}=3\Gamma/160$, and $\gamma_{78}=\Gamma/80$. Figure 7 shows the atomic population in the trapping state ($5S_{1/2}$, $F=2$, $m_F=1, 2$) as a function of $R_{\rm op2}$, provided that the probe beam power is kept unchanged. The horizontal red line is a reference when there is only a probe field. We see that the atomic population in trapping state increases with re-pump beam power increasing, e.g. for $R_{\rm op2}/R_{\rm op1}=1$ and 4, we have $[n(\text{black})-n(\text{red})]/n(\text{red})=62.3\%$ and 73.6%, respectively, which accord well with the experimental results.

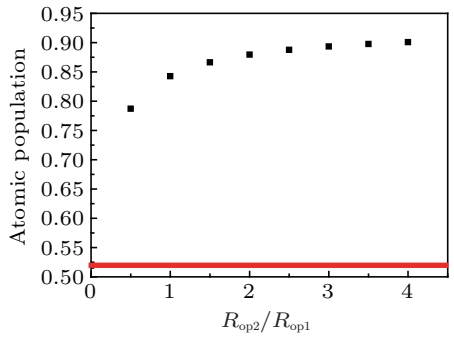


Fig. 7. (color online) Population versus normalized optical pumping rate in the system.

3. Conclusions

In this paper, we demonstrate an atomic magnetometer based on optical pumping theory, a magnetic resonance that is induced by a radio frequency field and dependent on the magnetic field strength. We show that the amplitude of magnetic field resonance signal can increase more than 55% using an additional re-pump beam, which makes the sensitivity of this magnetometer better. Using $5S_{1/2}$, $F=1\rightarrow 5P_{1/2}$, $F=2$ as a re-pump beam is superior to using $5S_{1/2}$, $F=1\rightarrow 5P_{1/2}$, $F=1$. We also investigate the relation between amplitude of the signal and re-pump laser power. It is found that the larger amplitude of the signal can be obtained with a higher re-pump laser power. Finally, in order to explain our results, we calculate the atomic population in the trapping states with rate equations. This type of magnetometer provides manifold applications such as in geophysical surveying, space science, nuclear magnetic resonance, non-destructive testing, medical diagnoses, gravitational wave detection, etc.

References

[1] Sarma B S P, Verma B K and Satyanarayana S V 1999 *Geophysics* **64** 1735

[2] Livanov M N, Kozlov A N, Sinelnikova S E, Kholodov J A, Markin V P, Gorbach A M and Korinewsky A V 1981 *Adv. Cardiol.* **28** 78

[3] Bison G, Wynands R and Weis A 2003 *Appl. Phys. B: Lasers Opt.* **76** 325
[4] Dehmelt H G 1957 *Phys. Rev.* **105** 1487
[5] Kominis I K, Kornack T W, Allred J C and Romalis M V 2003 *Nature* **422** 596
[6] Patton B, Versolato O, Hovde D C, Corsini E, Higbie J and Budker D 2012 *Appl. Phys. Lett.* **101** 083502
[7] Sternickel K and Braginski A 2006 *Supercond. Sci. Technol.* **19** S160
[8] Xu S, Yashchuk V V, Donaldson M H, Rochester S M, Budker D and Pines A 2006 *Proc. Natl. Acad. Sci. USA* **103** 12668
[9] Zivotskya O, Postavaa K, Krausb L, Jiraskovac Y, Juraszekd J, Teilletd J, Barcovaa K, Svece P, Janickovice D and Piatoraa J 2008 *J. Magn. Magn. Mater.* **320** 1535
[10] Bonavolonta C, Valentino M, Peluso G and Barone A 2007 *IEEE Trans. Appl. Supercond.* **17** 772
[11] Kuroda M, Yamanaka S and Isobe Y 2005 *NDT& E International* **38** 53
[12] Tralshawala N, Claycomb J and Miller J 1997 *Appl. Phys. Lett.* **71** 1573
[13] Zhang S L, Liu Y B, Zeng J, Wang Y L, Kong X Y and Xie X M 2012 *Acta Phys. Sin.* **61** 020701 (in Chinese)
[14] Gu H F, Cai W Y and Wei Y K 2012 *Chin. Phys. B* **21** 040702
[15] Huang K K, Li N and Lu X H 2012 *Chin. Phys. Lett.* **29** 100701
[16] Happer W 1972 *Rev. Mod. Phys.* **44** 169
[17] Bloom A L 1962 *Appl. Opt.* **1** 61
[18] Groeger S, Pazgalev A S and Weis A 2005 *Appl. Phys. B: Lasers Opt.* **80** 645
[19] Wieman C and Hansch T W 1976 *Phys. Rev. Lett.* **36** 1170
[20] Liu G and Gu S 2010 *J. Phys. B: At. Mol. Opt. Phys.* **43** 035004
[21] Seltzer S 2008 "Developments in Alkali-Metal Atomic Magnetometry" Ph. D. Thesis (New Jersey: Princeton University)
[22] Drake G W F (ed.) 2006 *Handbook of Atomic, Molecular, and Optical Physics* (New York: Springer-Verlag) p. 1005